Nonlinear self-defocusing in doped silica sono-gels

Rocío Ramos
Facultad de Ciencias, Departamento de Fisica de la Materia Condensada, Universidad de Cádiz, 11510 Puerto Real, Spain

Paul Michael Petersen,[a] Per Michael Johansen, and Lars Lindvold
Optics and Fluid Dynamics Department, Risø National Laboratory, DK-4000 Roskilde, Denmark

Mila Ramírez and Eduardo Blanco
Facultad de Ciencias, Departmento de Fisica de la Materia Condensada, Universidad de Cádiz, 11510 Puerto Real, Spain

(Received 6 December 1996; accepted for publication 17 March 1997)

Experiments with nonlinear self-refraction of Gaussian laser beams in silica sono-gels doped with copper tetrasulfonated phthalocyanine are reported. The propagation of laser beams inside nonlinear sol-gel samples with different Cu-phthalocyanine concentrations has been monitored by measuring the spatial beam profile in the near field and in the far field behind the sample. The experimental results are analyzed by a new simple theoretical approach, in which we assume that the incident Gaussian beam induces a phase shift that varies as a Gaussian function of the beam radius. The beam propagation behind the sample is determined by the Huygens–Fresnel integral formalism. By solving the Huygens–Fresnel integral, analytical expressions for the spatial beam profile in both the near field and the far field after the nonlinear sample are obtained. Experiments are carried out with a diode pumped frequency doubled Nd–YAG laser at 532 nm. We obtain very large third-order nonlinearities in these doped sol-gel samples at temperatures just above room temperature. When we compare the predictions of the theory with the experimental data, we find experimental values of the nonlinear third-order susceptibility up to -2.3×10^{-4} esu. © *1997 American Institute of Physics.* [S0021-8979(97)05012-3]

I. INTRODUCTION

Organic dyes with extensively delocalized π-electron systems can exhibit relatively large third-order nonlinear susceptibility $\chi^{(3)}$ and fast response times.[1–4] The nonlinear optical properties of these organic molecules with a good singlet–triplet transfer are based on the long lifetime of the lowest lying triplet state.[5] Saturable absorption in a material facilitates an intensity dependent change in the index of refraction. By optical excitation, electrons are transferred from the ground state S_0 to the first excited singlet state of the molecules S_1. From this state excited electrons can be transferred to the lowest triplet state T_1 by a process referred to as intersystem crossing (ISC). If the energy differences between T_1 and S_1 is small, ISC will take place in the reverse and cause the excited triplet state T_1 to be converted into an excited singlet state S_1 that relaxes into its ground state S_0 by emission of light. This process is known as delayed fluorescence. If the electrons remain in the excited triplet state T_1 the intensity required for saturable absorption will be significantly reduced. As the nonlinear susceptibility is inversely proportional to the saturation intensity, the magnitude of the nonlinear susceptibility in these materials becomes large. When the dye is held rigidly in a solid matrix, many of the mechanisms that quench the triplet state are reduced by the dye/matrix interaction. Consequently, the optical nonlinearity of the material is increased.[6]

Nonlinear optical properties of phthalocyanine planar organic molecules with an extensively delocalized two-dimensional conjugated π-electron system[7–11] have been measured in films on silica substrate[12] or in solutions.[13] Nevertheless, to the best of our knowledge, phthalocyanine molecule encapsulation in a solid silica matrix has not been reported in the literature. This material is very interesting for nonlinear integrated optics applications. While typical melt glasses require processing temperatures that could cause the decomposition of most organic compounds, the sol-gel method provides a low temperature route. Such a method makes it possible to trap organic molecules at room temperature whereby a transparent and homogeneous material with appropriate optical quality is obtained.[14] It is possible to prepare composites with different phthalocyanine concentrations and, consequently, to tailor the material optical behavior and the textural properties of these composites.

In the present work, silica sono-gels doped with commercial copper tetrasulfonated phthalocyanine (CuPc) have been prepared. The resulting composites exhibit large intensity dependent refractive index changes due to the presence of phthalocyanine molecules.

II. SAMPLE PREPARATION AND CHARACTERIZATION

The CuTSPc-silica-sono-xerogel composites we use here are prepared by hydrolysis and polycondensation of tetramethoxysilane (TMOS) with CuPc in an aqueous solution.

In order to obtain monolithic samples, formamide was used to control the drying process chemically. The additive, formamide, was added in a molar ratio of 3:1 (formamide/TMOS ratio). The water utilized to invoke the hydrolysis was acidified by nitric acid to a $p\mathrm{H}=2$ or to a $p\mathrm{H}\ll1$ (1 ml

[a]Electronic mail: paul.michael.petersen@risoe.dk

 0021-8979/97/81(12)/7728/6/$10.00 © 1997 American Institute of Physics

Downloaded¬06¬Oct¬2006¬to¬150.214.231.66.¬Redistribution¬subject¬to¬AIP¬license¬or¬copyright,¬see¬http://jap.aip.org/jap/copyright.jsp

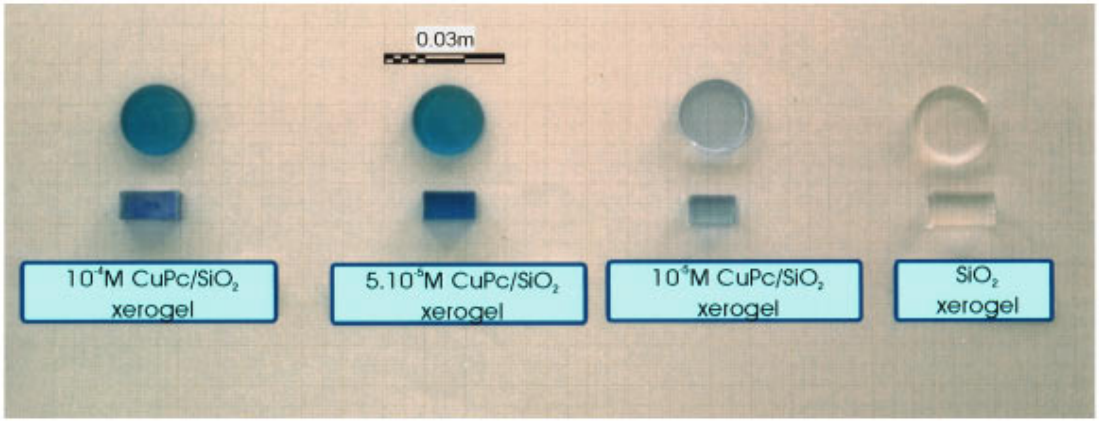

FIG. 1. Photograph of the Cu-phthalocyanine sol-gel samples with different concentrations of Cu-phthalocyanine ranging from 0 to 10^{-4} M.

nitric acid/9 ml water) and was added in a molar ratio of either 6:1 or 10:1 (H_2O/TMOS ratio). The acidified water contained CuPc in concentrations of 10^{-4}, 5×10^{-5}, and 10^{-5} M.

When formamide and acidified water had been mixed with the alkoxide, the solution was sonicated, as described elsewhere,[15] with the result that the mixture became transparent. This mixture is then left for gelling. Prior to our experimental investigation of self-refraction of laser beams, the transparent blue gels (Pc-xerogels) have been aged for one week and dried at room temperature for three weeks.

Photographs of the undoped sol-gel sample and samples doped with 10^{-4}, 5×10^{-5}, and 10^{-5} M Cu-phthalocyanine are shown in Fig. 1. Absorption spectra experiments have been carried out by a UV-visible spectrophotometer. The absorption spectra of these samples are shown in Fig. 2 for sol-gel samples with 10^{-5}, 5×10^{-5}, and 10^{-4} Cu-phthalocyanine.

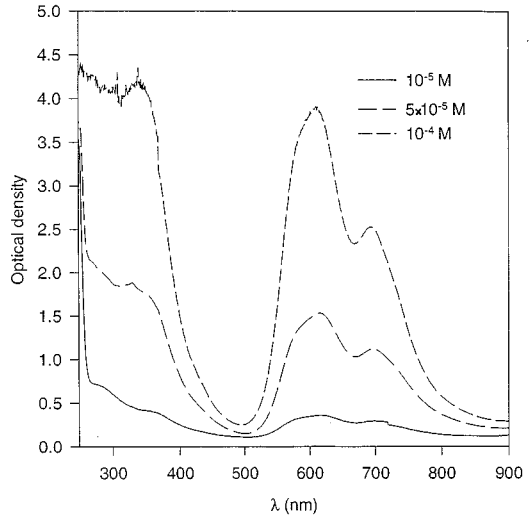

FIG. 2. The absorption spectra for sol-gel samples with 10^{-5}, 5×10^{-5}, and 10^{-4} M Cu-phthalocyanine. The absorption spectra are carried out by a UV-visible spectrophotometer.

III. SELF-REFRACTION OF GAUSSIAN BEAMS

Self-focusing and self-defocusing are well known processes in nonlinear optics.[16,17] These processes take place when Gaussian laser beams propagate in media where the refractive index varies with optical intensity. There have been many approaches to the theories of self-focusing and self-defocusing.[19–22] Some years ago these effects were considered detrimental beam distortion effects. Today, however, the nonlinear effects have become important for calculating nonlinear material parameters such as the magnitude of the third-order nonlinear susceptibility and the sign of the refractive index change. In general, the self-refraction problem cannot be solved analytically. Yet in this article we outline a new simple analytical approach to self-refraction of Gaussian laser beams inside a nonlinear medium. The model is based on the simplified assumption that the beam intensity profile always remains Gaussian inside the nonlinear material. The theory can be applied to any Kerr-like material and here it is used to calculate the magnitude of the third-order nonlinear susceptibility of phthalocyanine/SiO_2 composites. Comparing theory with experiments it is important that the experimental conditions fulfill the basic assumptions of the theory. These assumptions are (1) the incident beam is a plane wave and (2) the intensity profile in the nonlinear material is Gaussian. The latter assumption is fulfilled when the refractive index change in the sample is not too high.

In the theory we will assume that the laser beam inside the nonlinear material induces a phase shift that varies as a Gaussian function of the beam radius. This assumption is valid for Kerr-like media with a Gaussian intensity profile inside the material. The beam propagation after the nonlinear material is determined using a Huygens–Fresnel integral approach. We solve the integral and obtain an analytical expression for the spatial beam profile at an arbitrary position after the sample. The configuration for the self-refraction setup is shown in Fig. 3. The nonlinear material of thickness d is fixed between $z=-d$ and $z=0$, and the electric field is to be determined in the output observation plane (x_0,y_0). The induced refractive index change in the nonlinear material is given by $n=n_0+\Delta n=n_0+n_2I$, where I is the total

Downloaded¬06¬Oct¬2006¬to¬150.214.231.66.¬Redistribution¬subject¬to¬AIP¬license¬or¬copyright,¬see¬http://jap.aip.org/jap/copyright.jsp

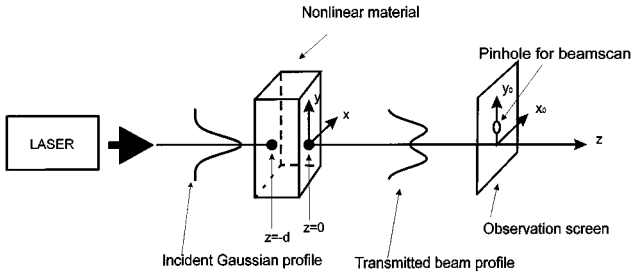

FIG. 3. Configuration of the self-refraction setup. The incident Gaussian intensity profile is distorted by the nonlinear material. The distorted intensity profile is monitored at the observation screen.

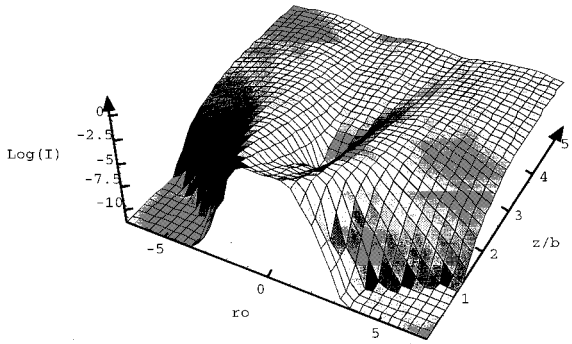

FIG. 4. The theoretical plot of the intensity profile vs the transverse spatial coordinate r_0 in units of $\lambda/(\pi w)$ and the distance z behind the nonlinear sample when $\beta_2=-4.0$. The twin peaks in the near field $z/b \ll 1$ develop into one central peak and two off-axis peaks in the far field ($z/b>3$). Note $b=\pi w^2/\lambda$ is the Rayleigh length.

optical intensity, n_0 is the linear refractive index, and n_2 is the nonlinear refractive index coefficient. The phase shift δ in the material is given by

$$\frac{\partial \delta(z,r)}{\partial z}=\frac{2\pi}{\lambda}\, n_2 I, \tag{1}$$

where z is the distance behind the sample, $r=(x^2+y^2)^{1/2}$ is the radial distance, and λ is the wavelength in vacuum. We assume that the intensity inside the sample remains Gaussian

$$I=I_0\, \exp\left(-\frac{r^2}{w^2}\right)\, \exp\left[-\alpha(z+d)\right], \tag{2}$$

where I_0 is the maximum incident intensity at $z=-d$, α is the linear absorption coefficient, and w is the beam spot size in the sample. Using Eq. (1) we can calculate the phase at the exit face of the nonlinear medium at $z=0$ from the following integral:

$$\begin{aligned}\delta(0,r)&=\frac{2\pi}{\lambda}\, n_2 I_0\, \exp\left(-\frac{r^2}{w^2}\right)\int_{z=-d}^{z=0} e^{-\alpha(z+d)}dz\\ &=\frac{2\pi}{\lambda}\, n_2 I_0\, \exp\left(-\frac{r^2}{w^2}\right)\frac{(1-e^{-\alpha d})}{\alpha}+\delta_0,\end{aligned} \tag{3}$$

where δ_0 is the initial phase of the optical field at $z=-d$. The electric field at the exit face of the material is consequently given by

$$E(0,r)=\beta_1\, \exp\left(-\frac{r^2}{2w^2}\right)\, \exp\left[-i(\delta_0+\beta_2 e^{-r^2/w^2}\right], \tag{4}$$

where $\beta_1=(2I_0/n_0\epsilon_0 c)^{1/2}$, $\beta_2=(1-e^{-\alpha d})I_0 n_2 2\pi/(\lambda\alpha)$, ϵ_0 is the vacuum permittivity, and c is the velocity of light in vacuum. The electric field in the observation plane can now be determined by the Huygens–Fresnel formalism[23]

$$\begin{aligned}E(z,r_0)=&\frac{2\pi\, \exp\left(ikz+\frac{\pi}{z\lambda}r_0^2\right)}{iz\lambda}\\ &\times\int_0^\infty E(0,r)J_0\left(2\pi\frac{r_0}{z\lambda}r\right)\, \exp\left(i\frac{\pi}{z\lambda}r^2\right)rdr,\end{aligned} \tag{5}$$

where we have introduced the cylindrical coordinates $(x,y)=r(\cos\varphi,\ \sin\varphi)$ and $(x_0,y_0)=r_0(\cos\psi,\ \sin\psi)$. Equation (5) determines the beam propagation after passage of the nonlinear medium, and this integral can be solved provided a Taylor expression of the phase part $e^{i\delta}$ of E in terms of $\exp[-(r/w)^2]$ is made, i.e.,

$$e^{i\delta(z,r,t)}=e^{-i\delta_0}\sum_{n=0}^{\infty}\frac{(-i\beta_2)^n}{n!}\exp\left(-n\frac{r^2}{w^2}\right). \tag{6}$$

By using the relation[24] $\int_0^\infty e^{-a^2t^2}J_0(bt)dt=\exp[-b^2/(4a^2)]/2a^2$ in Eqs. (5) and (6), we obtain the final expression

$$\begin{aligned}E(z,r_0)=&\frac{2\pi\, \exp\left(ikz+\frac{\pi}{z\lambda}r_0^2\right)}{iz\lambda}\,\beta_1 e^{-i\delta_0}\\ &\times\sum_{n=0}^{\infty}\int_0^\infty\frac{(-i\beta_2)^n}{n!}\exp\left[-(n+1/2)\frac{r^2}{w^2}\right.\\ &\left.+i\frac{\pi}{z\lambda}r^2\right]J_0\left(2\pi\frac{r_0 r}{z\lambda}\right)rdr\\ =&\frac{2\pi\, \exp\left[i\left(kz+\frac{\pi}{z\lambda}r_0^2\right)\right]}{iz\lambda}\beta_1 e^{-i\delta_0}\\ &\times\sum_{n=0}^{\infty}\frac{(-i\beta_2)^n}{2n!}w_n^2\, \exp\left[-\left(\pi\frac{r_0}{z\lambda}w_n\right)^2\right],\end{aligned} \tag{7}$$

where

$$w_n^2=\frac{w^2}{n+1/2+i\frac{\pi w^2}{\lambda z}} \tag{8}$$

is the square of the complex beam radius. Equation (7) is the main result of this section and from that equation we can calculate the intensity profiles at arbitrary positions behind the nonlinear sample.

In self-refraction experiments it is important to distinguish between the near field and the far field behind the nonlinear medium. In the near field the distance from the sample is smaller than the Rayleigh length $b=\pi w^2/\lambda$ and in the far field the distance from the sample is much larger than

Downloaded¬06¬Oct¬2006¬to¬150.214.231.66.¬Redistribution¬subject¬to¬AIP¬license¬or¬copyright,¬see¬http://jap.aip.org/jap/copyright.jsp

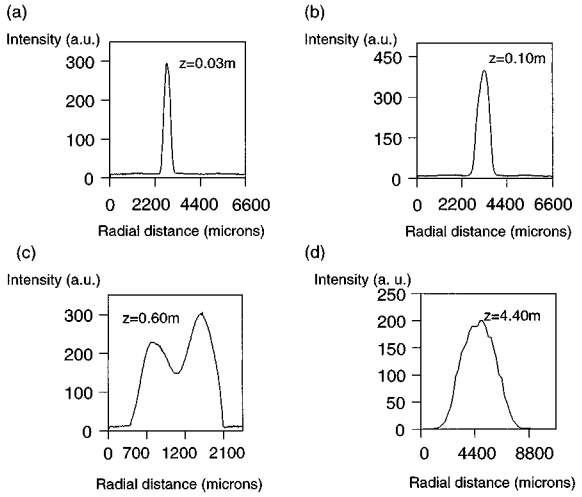

FIG. 5. Beam intensity profiles at different distances; (a) $z=0.03$ m, (b) $z=0.10$ m, (c) $z=0.60$ m, (d) $z=4.40$ m, and (e) after passage through a 5×10^{-5} M Pc xerogel when the incident intensity is $I=2.0\times10^{5}$ W/m^2.

b. In Fig. 4 a theoretical plot of the laser beam intensity versus the transverse spatial coordinate r_0 and the distance z behind the nonlinear sample is shown, calculated from Eq. (7). In the near field, $z/b<1$, self-defocusing with two peaks and a minimum in the center of the beam is shown. In the far field, $z/b>3$, however, an intensity profile has one central peak and two off-axis peaks. The parameters used in Fig. 4 are $\beta_1=0.5$ and $\beta_2=(1-e^{-\alpha d})I_0 n_2 2\pi/(\lambda\alpha)=-4.0$.

IV. EXPERIMENTS

In the experimental part of the present article we have investigated the propagation of laser beams inside different sol-gel samples doped with 10^{-5}, 5×10^{-5}, and 10^{-4} M Cu-phthalocyanine. As mentioned earlier, the absorption spectra of these samples are shown in Fig. 2.

Self-defocusing experiments have been performed with a frequency doubled Nd–YAG at $\lambda=532$ nm. A laser beam with Gaussian intensity profile is incident on the sample at normal incidence. The spatial beam profile of the transmitted intensity has been monitored by scanning a 25 μm pinhole across the beam as shown in Fig. 3. The purposes of the experiments are (i) to investigate the nonlinear self-refraction in sol-gel samples with different phthalocyanine concentrations and (ii) to apply the theory from Sec. III to determine the third-order susceptibility. When we apply the theory, it is important to check that the intensity profile remains Gaussian inside the sol-gel sample. This is verified experimentally by monitoring the beam profile just behind the sample ($z\ll b$). The assumption of a Gaussian intensity profile is valid only when the incident intensity level and the phthalocyanine concentration are not too high.

It is possible to distinguish self-focusing from self-defocusing in the near field. In the far field, however, there is competition between diffraction and nonlinear refraction, and the spatial beam profiles of self-focusing and self-defocusing are almost identical. Thus, in order to gain information in both the near field and the far field, the spatial beam profiles have been monitored at distances of $z=10$ cm (the near field), $z=60$ cm, and $z=440$ cm (the far field) behind the samples. The experiments allow us to determine if the self-refraction in the sol-gel samples originates from self-focusing or from self-defocusing and to determine the experimental value of the nonlinear refractive index n_2.

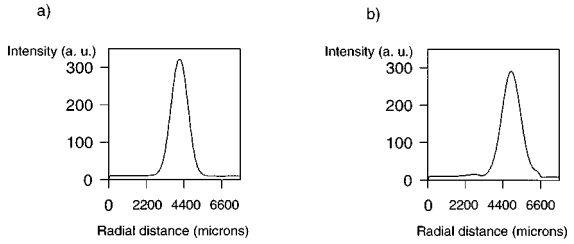

FIG. 6. Beam intensity profile at $z=0.60$ m. (a) Without any sample and (b) behind a SiO_2/xerogel sample without phthalocyanine.

Figures 5(a)–5(d) show the experimental spatial beam profiles at different distances of $z=0.03$, 0.10, 0.60, and 4.40 m, respectively, for an incident intensity of $I=2.00\times10^{5}$ W/cm^2. Although the intensity profile is Gaussian at $z=0.03$ m and $z=0.10$ m behind the sample, a minimum appears when the distance $z=0.60$ m as can be seen in Fig. 5(c). This central intensity minimum is not observed in the far field, where the distance is further increased. Figure 5(c) shows clearly that the nature of the nonlinear self-refraction

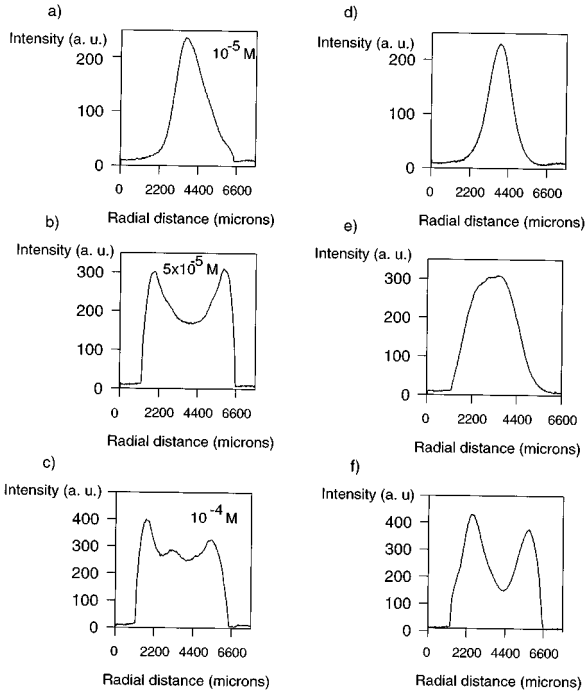

FIG. 7. Beam profiles obtained at $z=0.60$ m. (a)–(c). For Pc-xerogels with three different phthalocyanine concentrations when the incident intensity is $I=2.0\times10^{5}$ W/m^2, and (d)–(f) for a 5×10^{-5} M Pc-xerogel at three different incident intensities, (d) $I=3.36\times10^{4}$ W/m^2, (e) $I=8.29\times10^{4}$ W/m^2, and (f) $I=2.0\times10^{4}$ W/m^2. The self-defocusing effect becomes more pronounced as the Pc concentration or the incident intensity increases.

Downloaded¬06¬Oct¬2006¬to¬150.214.231.66.¬Redistribution¬subject¬to¬AIP¬license¬or¬copyright,¬see¬http://jap.aip.org/jap/copyright.jsp

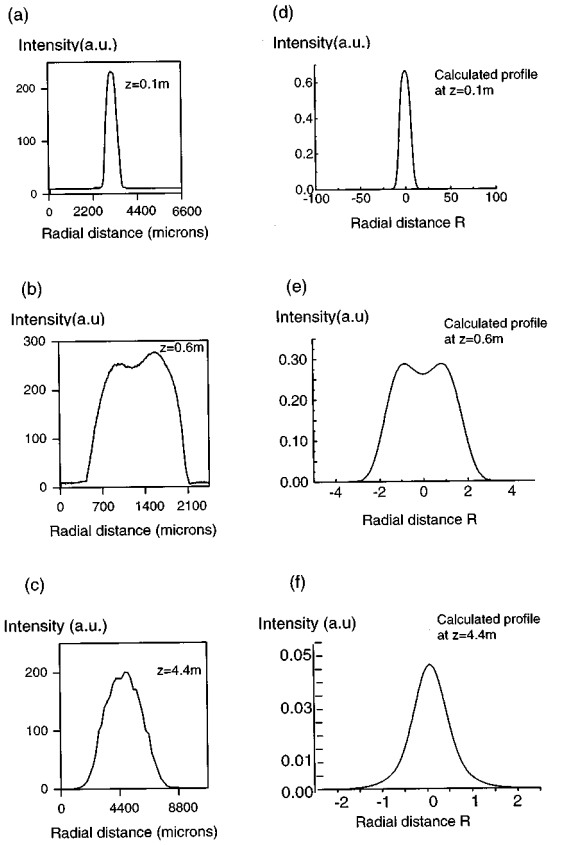

FIG. 8. Fitting between experimental (a)–(c) and theoretical (d)–(f)beam profiles for a Pc-xerogel that contains a phthalocyanine concentration of 10^{-5} M. The parameters are (a) and (d) $z=0.10$ m, (b) and (e) $z=0.60$ m, and (c) and (f) $z=4.40$ m. The theoretical curves are obtained using $\beta_2=-1.4$ and $I=4.82\times10^5$ W/m^2 and the radial distance in these curves is given by $R=w\pi r_0/(z\lambda)$.

is defocusing. This defocusing effect has been observed for all our phthalocyanine doped xerogel samples when the 532 nm wavelength laser was used. Sometimes, however, when the incident intensity or the Pc concentrations were too low, it was not possible to observe the self-defocusing. Furthermore, the self-defocusing effect is not observed when the Pc-silica-xerogel is replaced by a silica-xerogel without phthalocyanine. This fact is shown in Fig. 6(b) where even for a high incident intensity level of $I=1.36\times10^6$ W/cm^2 we obtain almost the same transmitted intensity profile as that measured without any sample present, see Fig. 6(a). The profiles in Fig. 6 are obtained at $z=0.60$ m after the samples. This obviously indicates that the self-refraction measured in Fig. 5 is solely caused by the presence of phthalocyanine in

TABLE I. The nonlinear refractive index change and the nonlinear susceptibility for different concentrations of Cu-phthalocyanine in sol-gel.

Phthalocyanine concentration (M)	Incident intensity (W m^{-2})	Coefficient β_2	n_2 (m^2 W^{-1})	$\chi^{(3)}$ (C^{2}N^{-2})
10^{-5}	$I=4.82\times10^5$	-1.4	-3.94×10^{-11}	-2.20×10^{-13}
5×10^{-5}	$I=8.29\times10^4$	-1.5	-3.12×10^{-10}	-1.74×10^{-12}
10^{-4}	$I=8.29\times10^4$	-2	-5.68×10^{-10}	-3.17×10^{-12}

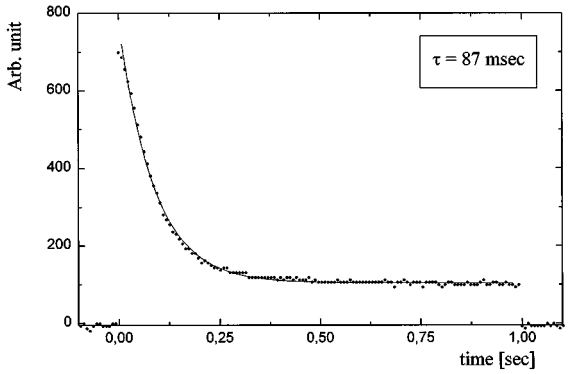

FIG. 9. The time response of the nonlinear self-refraction in a sol-gel sample with 5×10^{-5} M phthalocyanine. The transmitted intensity from a 1 mm pinhole is shown.

the samples. These organic molecules can induce the third-order nonlinear optical properties in the sample due to their delocalized conjugated π-electron system.[25,26]

Figure 7 shows the beam intensity profiles for different Pc concentrations [Figs. 7(a)–7(c)] and for several incident intensities [Figs. 7(d)–7(f)] for the same distance $z=0.60$ m after the samples. It is seen that the defocusing in Pc-xerogel samples is strongly dependent on the phthalocyanine concentration as well as on the incident intensity.

Although samples prepared with different amounts of hydrolysis water and different pHs have been studied, their experimental behavior has been found to be identical to that found for samples containing the same Pc concentration independent of the water concentration and of the pH level. Therefore, we conclude that the self-refraction is independent of the pH level.

When we compare the experimental profiles with the theory in Sec. III, it is possible to estimate a value for the nonlinear refractive index coefficient n_2 and, hence, for the third-order nonlinear susceptibility $\chi^{(3)}$ for the different samples. The nonlinear refractive index coefficient is determined from the expression

$$n_2=\frac{\beta_2\lambda\alpha}{2\pi I_0(1-e^{-\alpha d})}, \tag{9}$$

where the absorption coefficient α of the sample is obtained from the absorption spectra.

In Kerr-like media the refractive index for small nonlinearities is approximately given by

$$n\cong Re\chi^{(1)}+Re\chi^{(3)}\frac{I}{\epsilon_0 n_0^2 c}, \tag{10}$$

where the relation $I=\frac{1}{2}\epsilon_0 n_0 cE^2$ has been used. Comparing this expression with $n=n_0+n_2I$, a relation between n_2 and $\chi^{(3)}$ is found

$$Re\chi^{(3)}=n_2\epsilon_0 n_0^2 c, \tag{11}$$

where n_0 is the linear refractive index of the samples. Thus, estimated values of the third-order nonlinear susceptibility can be obtained from Eqs. (9) and (11).

In Figs. 8(a)–8(c) the experimental curves for 10^{-5} M Pr concentration and $z=0.10$, 0.60, and 4.40 m, respec-

Downloaded¬06¬Oct¬2006¬to¬150.214.231.66.¬Redistribution¬subject¬to¬AIP¬license¬or¬copyright,¬see¬http://jap.aip.org/jap/copyright.jsp

tively, are shown. The beam spot size on the sol-gel sample is $w=320$ μm in these experiments and, consequently, the Rayleigh length is $b=0.60$ m. In Figs. 8(d)–8(f) the corresponding theoretical curves obtained from Eq. (7) are shown. The functional shape of the beam intensity profiles gives a very accurate measure for the nonlinear coefficient β_2. The best fit between experimetnal curves and theoretical curves is obtained for $\beta_2=-1.4$. From this value of β_2 we can calculate a third-order nonlinear susceptibility $\chi^{(3)}=-2.20\times10^{-13}$ $N^{-2}C^2$. For an incident intensity $I=8.29\times10^4$ Wm^{-2} we have furthermore preformed the same experiment as the one in Fig. 8 when the phthalocyanine concentration was 5×10^{-5} and 10^{-4} M. Comparing these experimental curves for 5×10^{-5} and 10^{-4} M with the theory from Sec. III we find that the best agreement is obtained for $\beta_2=-1.5$ and $\beta_2=-2$, respectively. From the theoretical values of β_2, we have, using Eqs. (9) and (11), calculated the nonlinear intensity coefficient n_2 and the corresponding value of the third-order susceptibility $\chi^{(3)}$. The results are summarized in Table I together with the results from Fig. 8. In the calculations we have used $n_0=1.45$ and $d=6.5\times10^{-3}$ m. The magnitude of n_2 and $\chi^{(3)}$ increase as the Pc concentration in xerogels is increased. The nonlinear susceptibility is increased significantly—by one order of magnitude—as the phthalocyanine concentration is changed from 10^{-5} to 5×10^{-5} M. In Table I we obtain large values of n_2 and $\chi^{(3)}$. At 10^{-4} M phthalocyanine we obtain $\chi^{(3)}=-3.17\times10^{-12}$ C^2N^{-2}. This extremely large value of the nonlinear susceptibility is equivalent to -2.3×10^{-4} esu.

When the intensity is further increased, beyond 10^5 Wm^{-2}, the profiles are extremely distorted for high phathalocyanine concentrations ($>10^{-4}$ M) and it is difficult to find an appropriate fit. This may be due to the fact that the initial assumption that the beam remains Gaussian is violated at high incident intensities for the high molecule concentration case.

Finally, in Fig. 9 we have monitored the time constant of the nonlinear material response of a sol-gel sample with a 5×10^{-5} M phthalocyanine concentration. A pinhole with a diameter of 1 mm was placed $z=0.31$ m behind the sample in the center of the transmitted beam, and the time response was monitored when a beam shutter was placed in front of the sample. At $t=0$ s the shutter is opened electronically and the transmitted intensity from the pinhole is monitored by a semiconductor detector. In Fig. 9 the filled circles correspond to the experimental values and the dashed curve corresponds to a theoretical exponential function. The best fit to the experimental curve is obtained when the time constant of the exponential function equals 87 ms.

V. CONCLUSIONS

The propagation of a Gaussian laser beam inside sol-gel samples with different phthalocyanine concentrations, has been investigated. Experiments carried out with a Nd–YAG laser at 532 nm show strong self-defocusing for samples that contain Cu-phthalocyanine concentrations between 10^{-5} and 10^{-4} M. The experimental results are compared with a theory based on the Huygens–Fresnel propagation formalism. Good agreement between theory and experiment is found for sol-gel samples with low concentrations of phthalocyanine. For high concentrations and high incident optical intensities, deviation between theory and experiment takes place. When we compare theory and experiments, we find third-order susceptibilities up to -2.3×10^{-4} esu at 10^{-4} M phthalocyanine. From a time resolved self-defocusing experiment we determine a time constant of 87 ms for the nonlinear material response.

[1] B. I. Greene, J. Orenstein, and S. Schmitt-Rink, Science **247**, 679 (1990).
[2] J. S. Shink, J. R. Lindle, F.J. Bartoli, Z. H. Kufafi, and A. W. Snow, *Materials for Nonlinear Optics*, edited by S. R. Marder, J. E. Sohn, and G. D. Stucky (American Chemical Society, Washington, DC, 1991), p. 626.
[3] J. Zyss, *Molecular Nonlinear Optics*, edited by J. Zyss (Academic, New York, 1993).
[4] P. N. Prasad and D. J. Williams, *Introduction to Nonlinear Effects in Molecules and Polymers* (Wiley, New York, 1991).
[5] C. Sanchez, ''Materiaux Pour L'Optique Elabores Par Le Procede Sol-Gel,'' Ecole d'Ete Oleron (1991).
[6] R. Reisfeld, J. Non-Cryst. Solids **121**, 254 (1990).
[7] C. C. Leznoff and A. B. P. Lever, *Phthalocyanines, Properties, and Applications* (VCH, New York, 1989), Vols. 1–3.
[8] Z. Z. Ho, C. Y. Ju, and W. M. Hetherington, J. Appl. Phys. **62**, 716 (1987).
[9] M. Hosoda, T. Wada, A. Yamada, A. F. Garito, and H. Sasabe, Jpn. J. Appl. Phys. **30**, L1486 (1991).
[10] M. Hosoda, T. Wada, A. Yamada, A. F. Garito, and H. Sasabe, Jpn. J. Appl. Phys. **30**, 1715 (1991).
[11] M. A. Díaz García, I. Ldoux, J. A. Duro, T. Torres, F. Agulló-López, and J. Zyss, J. Phys. Chem. **98**, 8761 (1994).
[12] D. V. Rao, F. J. Aranda, J. F. Roach, and D. E. Remy, Appl. Phys. Lett. **58**, 1241 (1991).
[13] T. H. Wei, D. J. Hogan, M. J. Sence, E. W. Van Stryland, J. W. Perry, and D. R. Coulter, Appl. Phys. B **54**, 46 (1992).
[14] M. Ocaña, D. Levy, and C. J. Serna, J. Non-Cryst. Solids **147&148**, 621 (1992).
[15] N. de la Rosa Fox, L. Esquivias, and J. Zarzycki, J. Non-Cryst. Solids **121**, 211 (1990).
[16] Y. R. Shen, *Principles of Nonlinear Optics* (Wiley, New York, 1984).
[17] A. Yariv, *Quantum Electronics* (Wiley, New York, 1989).
[18] P. R. Longaker and M. M. Litvak, J. Appl. Phys. **40**, 4033 (1969).
[19] Y. R. Shen, Prog. Quantum Electron. **4**, 1 (1975).
[20] S. Akhmanov, R. Khokhlov, and A. Sukhorukov, *Laser-Handbook*, edited by F. T. Arechi and E. O. Schulz-Du Bois (North Holland, Amsterdam, 1972), p. 1151.
[21] D. Waire, B. S. Wherret, D. A. B. Miller, and S. D. Smith, Opt. Lett. **4**, 331 (1979).
[22] E. Van Stryland, H. Vanherzeele, H. Woodal, M. Soileau, A. L. Smirl, S. Guha, and T. Boggess, Opt. Eng. (Bellingham) **24**, 613 (1985).
[23] M. Nieto-Vesperinas, *Scattering and Diffraction in Physical Optics* (Wiley, New York, 1991).
[24] M. Abramowitz and I. A. Stegun, *Handbook of Mathematical Functions* (Dover, New York, 1970).
[25] H. S. Nalwa, T. Saito, A. Kakuta, and T. Iwayanagi, J. Phys. Chem. **97**, 10 515 (1993).
[26] J. Perry, K. Mansour, S. Marder, K. J. Perry, D. Alvarez, and Y. Choongo, Opt. Lett. **19**, 625 (1994).

Downloaded¬06¬Oct¬2006¬to¬150.214.231.66.¬Redistribution¬subject¬to¬AIP¬license¬or¬copyright,¬see¬http://jap.aip.org/jap/copyright.jsp